Why Do Self-Supervised Models Transfer? Investigating the Impact of Invariance on Downstream Tasks

Linus Ericsson
University of Edinburgh
linus.ericsson@ed.ac.uk

Henry Gouk
University of Edinburgh
henry.gouk@ed.ac.uk

Timothy M. Hospedales
University of Edinburgh,
Samsung AI Research, Cambridge
t.hospedales@ed.ac.uk

Abstract

Self-supervised learning is a powerful paradigm for representation learning on unlabelled images. A wealth of effective new methods based on instance matching rely on data-augmentation to drive learning, and these have reached a rough agreement on an augmentation scheme that optimises popular recognition benchmarks. However, there is strong reason to suspect that different tasks in computer vision require features to encode different (in)variances, and therefore likely require different augmentation strategies. In this paper, we measure the invariances learned by contrastive methods and confirm that they do learn invariance to the augmentations used and further show that this invariance largely transfers to related real-world changes in pose and lighting. We show that learned invariances strongly affect downstream task performance and confirm that different downstream tasks benefit from polar opposite (in)variances, leading to performance loss when the standard augmentation strategy is used. Finally, we demonstrate that a simple fusion of representations with complementary invariances ensures wide transferability to all the diverse downstream tasks considered.

1. Introduction

Self-supervised learning algorithms have made rapid progress in unsupervised representation learning, with performance approaching and sometimes surpassing that of supervised pre-training. In computer vision contrastive self-supervised methods driven by data augmentation have been particularly effective [7, 26]. Data augmentation applies synthetic class-preserving transformations to images during learning, to increase effective data volume and promote invariance to the augmentation distribution used [14, 49]. In self-supervised learning, many algorithms optimise representations so that individual images are similar to their augmented counterparts [9, 25], possibly while also being dif-

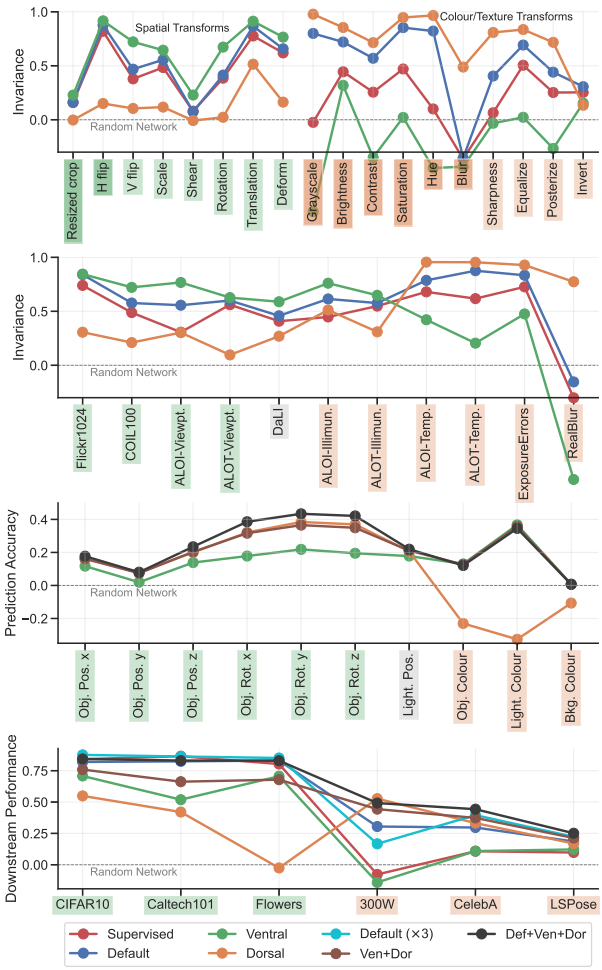

Figure 1. Our Ventral and Dorsal models lead to strong spatial and colour/texture invariance respectively, as measured by both synthetic (first row) and real-world (second row) transforms. Simple feature fusion (black) dominates individual pathways, as well as state of the art 'default' augmentation, providing more consistent performance across all downstream tasks (third and fourth row).

ferent to alternative distractor images [7, 26, 53]. This strategy of training a representation that achieves augmentation invariance along with instance sensitivity and has had wide success [18].

In this paradigm the properties and efficacy of the learned representation are largely determined by the augmentation distribution used during self-supervision. To this end a rough consensus has emerged among many state of the art methods as to a good default distribution that leads to strong performance on the downstream benchmarks, especially on the ubiquitous ImageNet object recognition benchmark [15]. For example, image cropping, flipping, colour perturbation and blurring, are widely applied [8, 18, 26].

However, if augmentation leads to invariance to the corresponding transformation, then we should ask whether our self-supervised algorithms provide the right invariances for diverse downstream tasks of interest? For example, while an object categorisation task might benefit from pose invariance, other tasks such as pose estimation may require strong spatial sensitivity. If different tasks require contradictory (in)variances, using a single default distribution for all may provide sub-optimal performance for some tasks.

To investigate this issue, we group augmentations into two categories that are loosely inspired by the two visual pathways of the brain [23, 34], namely the *ventral* pathway that focuses on recognition and the *dorsal* pathway that focuses on spatial and motion information. Using a representative state of the art contrastive learner MoCo-v2+ResNet50 [8], we train models exclusively with ventral-style and dorsal-style augmentations and compare them to the model produced by the default augmentation scheme. In particular, we evaluate their resulting invariances to synthetic and real-world transformations, as well as their performance on a suite of diverse real-world downstream tasks.

Based on the experimental design outlined above, we attempt to better understand *why contrastive self-supervised learning works?* by answering the following specific questions among others, with associated results summarised in Figure 1. **Q1** *Do neural networks trained contrastively with data augmentation lead to corresponding invariances in the learned features?* A1: Yes. Invariance to the specific augmentations used in training is very high, and moreover there is increased invariance to other transformations in the same (dorsal/ventral) family (Fig. 1, top, Table 2). While this is intuitive, it has never been directly verified or measured to our knowledge. **Q2** *Do learned invariances to synthetic transformations translate to invariance to real-world transformations?* A2: To some degree, yes. For example, ventral-style augmentations lead to increased invariance to transforms such as viewpoint, while dorsal-style augmentations lead to increased variance to transformations such as lighting colour, exposure and blur. Correspondingly, ventral-style augmentations lead to higher accuracy in estimating object colour, while dorsal-style augmentation lead to higher accuracy in estimating object pose. (Fig. 1 second and third row). This has not been measured before. **Q3** *Do different downstream tasks of interest benefit from different invariances?* A3: Yes. Across a suite of downstream tasks, we see that recognition-style tasks prefer a representation trained on default or ventral-style augmentations, while pose-related tasks benefit from dorsal-style augmentations. In particular, default augmentations [8] under-perform in pose-related tasks (Fig. 1 fourth row). **Q4** *Given that different tasks prefer polar-opposite augmentations, is there a simple way to achieve high performance across all tasks?* A4: Yes. Simple fusion of multiple representations tuned for different (in)variances leads to consistent strong performance across all tasks considered (Fig. 1 third and third fourth row, black line).

Table 1. Augmentations used during pre-training of our Ventral and Dorsal models, along with the standard default augmentations [8]. The color jitter augmentation is a combination of individual jitter in brightness, contrast, saturation and hue.

	Resized crop	Horizontal flip	Color jitter	Grayscale	Blur
Default	✓	✓	✓	✓	✓
Ventral	✓	✓			
Dorsal			✓	✓	✓

2. Related Work

Self-supervision in computer vision is now too a large topic to review here. Please see [19, 29] for excellent surveys. A key trend is that many highly successful methods rely on matching individual images with augmented versions of themselves, possibly against a background of distractor images. This includes most contrastive methods [6, 26], and some that are not typically considered contrastive [25, 57]. These have been understood [53] as making image features invariant to transformations used for training, while otherwise separating individual images. A key ambition of self-supervision research is for a single pre-trained feature to support diverse downstream tasks, and a common suite of augmentations has emerged to support this [8, 18]. However if data augmentation determines (in)variances, and different tasks require different (in)variances then a single augmentation distribution may not perform well on all tasks.

Building in Invariances Early work in feature engineering produced SIFT and SURF features that were designed to be invariant to various common transformations [56]. With the advent of deep learning, the focus shifted to enforcing feature properties via neural network architectures. For images, convolutional neural networks [21, 27, 33] have long been the go-to architecture because of their weight-sharing and spatial equivariance properties. Many other architec-

Table 2. ImageNet pre-trained ResNet50 with MoCo-v2 (200 epochs) evaluated on invariances to transforms on 1000 ImageNet validation images. Top group: Mahalanobis distance where a low value means strong invariance. Bottom group: cosine similarity in a normalised feature space where a value close to 1 means strong invariance. Column colours indicate the type of invariance evaluated and row colours indicate the augmentation expected to lead to high-performing specialised models. The broad agreement between the most invariant features (bold) and expectation (row colours) indicates that training with augmentations does tend to learn the corresponding invariances.

			Resized crop	H flip	V flip	Scale	Shear	Rotation	Translation	Deform	Grayscale	Brightness	Contrast	Saturation	Hue	Blur	Sharpness	Equalize	Posterize	Invert
Distance	↓	Random	69.40	34.14	35.35	67.03	69.57	71.65	56.33	65.28	22.81	73.25	59.03	46.63	42.39	49.17	52.59	27.46	27.46	32.88
		Supervised	**57.44**	12.33	24.07	40.37	63.93	47.67	22.51	34.25	19.87	40.43	37.05	26.61	35.95	54.92	42.15	17.44	22.74	27.32
		Default	58.72	9.92	21.30	35.75	56.58	43.49	16.45	30.16	7.78	26.07	25.66	12.17	13.72	65.84	31.07	12.81	17.95	**24.71**
		Ventral	59.43	**8.17**	**15.57**	**32.05**	**56.50**	**32.93**	**13.85**	**26.08**	26.58	46.25	61.67	39.34	47.33	63.37	48.83	25.41	38.46	28.95
		Dorsal	64.35	27.52	29.05	56.33	71.81	62.49	33.14	52.20	**2.57**	**19.71**	**22.84**	**6.98**	**5.77**	**30.38**	**16.86**	**9.55**	**12.18**	29.24
Similarity	↑	Random	0.03	0.56	0.54	0.16	0.04	0.07	0.40	0.20	0.81	0.17	0.52	0.59	0.60	0.48	0.51	0.68	0.70	0.52
		Supervised	0.18	0.92	0.71	0.57	0.11	0.43	0.87	0.69	0.81	0.54	0.64	0.79	0.64	0.29	0.55	0.84	0.77	0.64
		Default	0.19	0.95	0.75	0.63	0.11	0.45	0.92	0.72	0.96	0.77	0.79	0.94	0.93	0.29	0.71	0.90	0.83	**0.67**
		Ventral	**0.25**	**0.96**	**0.87**	**0.70**	**0.26**	**0.70**	**0.95**	**0.81**	0.65	0.43	0.35	0.60	0.42	0.25	0.50	0.69	0.62	0.59
		Dorsal	0.03	0.63	0.59	0.26	0.03	0.09	0.71	0.33	**1.00**	**0.88**	**0.86**	**0.98**	**0.99**	**0.73**	**0.91**	**0.95**	**0.91**	0.58

tures have been developed that capture different or more in-/equi-variances [10, 11, 46]. We focus on understanding invariances due to learning under data augmentation instead.

Data Augmentation Data augmentation is the process of transforming input data points to increase the diversity of the training set. It has become key to achieving state-of-the-art performance for supervised learning of CNNs in vision [13]. Despite its ubiquity in practice, theoretical understanding of data augmentation is weak. There is some evidence that CNNs can generalise learned translation invariance [3] to unseen data, but also that they retain information about absolute spatial locations of objects via boundary effects [31]. Tools have been developed to measure the learned invariance of features to transformed inputs [24].

Data augmentation has become even more vital in practical self-supervision as outlined earlier. However, understanding the role of data augmentation in self-supervision has lagged behind practical engineering lore. Self-supervised contrastive learners with strong augmentation have been shown to learn occlusion-invariant representations, but not to capture viewpoint and category instance invariance [44]. [54] study the theoretical effects of data augmentation on self-supervised contrastive learning. They argue that data augmentation decouples the sparse semantic information in the input from the dense noisy information and that only the sparse semantic information is relevant to solving the downstream target task. [52] study the effects of data augmentation on invariances and downstream performances using a synthetic task. They show that it is hard to define augmentations to enforce a specific invariance, that augmentations generally have wider invariance effects on groups of factors and that using multiple augmentations in conjunction reliably improves recognition performance. However they focus on object recognition in a synthetic dataset. We take a wider perspective and look at how augmentation impacts a wide variety of real-world transformations, and real-world downstream tasks. A related study to ours is [55], which proposes LooC as a self-supervised method that separates different types of information into different features, i.e. colour, orientation etc. However, they only evaluate the impact on recognition tasks. A major contribution of ours is to demonstrate how diverse downstream tasks benefit from different measured invariances.

Ventral-Dorsal Visual System A well established theory about mammalian vision holds that the visual cortex is composed of two functional pathways [23, 34]. The *ventral* stream deals with the "what" of object recognition; and the *dorsal* stream deals with the "where" of spatial and motion information. This decomposition into specialised models has been exploited in applications such as object detection [17] and semantic grasping [28] in robotics. At the intersection of neuroscience and self-supervised learning, [2] showed that a two branch neural network trained with the CPC [41] loss on videos leads to dorsal and ventral-like pathways emerging. Moreover, models of the dorsal stream based entirely on findings from neuroscience and phychophysics (i.e., without use of machine learning) have been shown to accurately estimate motion and depth from videos [12, 43].

We explore self-supervised learning with different data augmentations as a way of achieving similar multi-stream pathways in CNNs for vision. Current methods [6, 26] train representations for invariance to a single set of augmentations that aim to suffice for all tasks. But we show that this current practice is better optimised for the most popular downstream benchmark of object recognition, and poor for pose-related tasks. We will investigate a multi-stream architecture combining representations trained for different invariances, and show that it provides a more general purpose high performance feature for diverse downstream tasks.

3. Methods

3.1. Pre-Training Models

Our main focus is on analysing the properties of self-supervised models pre-trained with different augmentation strategies. In particular, we choose MoCo-v2 [8] as a representative self-supervised learner that is widely used and

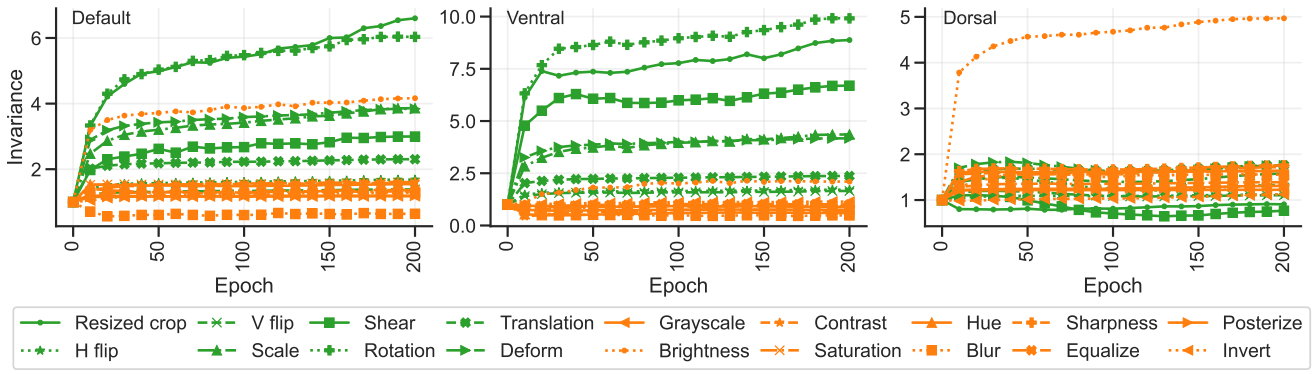

Figure 2. Invariances as measured by cosine similarity during pre-training. Different invariances are learned at different speeds. After 200 epochs many of the invariances are still steadily increasing, suggesting longer training helps achieve stronger invariances.

near state-of-the-art. MoCo-v2 matches images with their augmented counterparts, while using negative pairs in a contrastive loss to encourage feature dissimilarity between semantic objects, and to avoid features all collapsing to the same vector. We pre-train three models using MoCo-v2 [8] with ResNet50 architectures [27] on ImageNet [15] for 200 epochs.

- **Default** The default [6–8, 25, 35] model uses the standard array of data augmentations, which includes crops, horizontal flips, color jitter, grayscale and blur.
- **Ventral** The ventral model uses only the spatial subset of default augmentations, including crops and horizontal flips. By learning to be invariant to these spatial transformations, the model has to put larger focus on colour and texture, mirroring the *ventral* pathway.
- **Dorsal** The dorsal model uses only the appearance-based augmentations of color jitter, grayscale and blur. This model mirrors the *dorsal* pathway.

As baselines, we also compare a CNN with **Random** weights, and one pre-trained by **Supervised** learning. The details on the augmentations used in pretraining each model is summarised in Tab. 1.

3.2. Measuring Invariances

A key contribution of this paper is measuring the degree of invariance to various synthetic and real-world transformations. Previous studies have focused on measuring invariance at the neuronal level [24]. We consider instead the invariance properties of entire feature vectors under input transformations. To this end we explore two metrics.

Mahalanobis Distance A vector can be said to be invariant to a transformation if it remains unchanged after applying that transformation. We can measure the invariances of a feature extractor model by looking at how much its feature vectors change under different transformations. Given a pre-trained feature extractor f, whose feature space has a covariance of $\mathbf{\Sigma}$, a transformation t_ϕ parameterised by ϕ and an image x, we compute the variance of f to transformation t_ϕ as the Mahalanobis distance

$$l_f^{t_\phi}(x) = \sqrt{\Big(f(x) - f(t_\phi(x))\Big)\mathbf{\Sigma}^{-1}\Big(f(x) - f(t_\phi(x))\Big)^T} \tag{1}$$

$$= \|Gf(x) - Gf(t_\phi(x))\|_2 \tag{2}$$

where $\mathbf{\Sigma}^{-1} = GG^T$, and G can be computed using the Cholesky decomposition.

Cosine Similarity Alternatively, we can measure the angle instead of the distance by first standardising the vectors using the mean feature, $\bar{f}$, of f and G, giving us

$$z = G\Big(\bar{f} - f(x)\Big), \tag{3}$$

$$z_{t_\phi(x)} = G\Big(\bar{f} - f(t_\phi(x))\Big), \tag{4}$$

and then using cosine similarity to measure the angle between features, giving us an invariance measure of

$$l_f^{t_\phi}(x) = \frac{z \cdot z_{t_\phi(x)}}{\|z\|\,\|z_{t_\phi(x)}\|}. \tag{5}$$

The distance or similarity is computed over a range of transformation parameters, $\phi \in \Phi$—e.g. from $0°$ to $360°$ for rotation. Additionally, we average over all images in a dataset D. The global measurement is then

$$L_f^{T_\Phi}(D) = \frac{1}{|D||\Phi|}\sum_{x\in D}\sum_{\phi\in\Phi} l_f^{t_\phi}(x), \tag{6}$$

where $T_\Phi = \{t_\phi\}_{\phi\in\Phi}$. A model with zero Mahalanobis distance (variance) to a transformation is invariant to it. Likewise, a model with maximum cosine similarity is invariant.

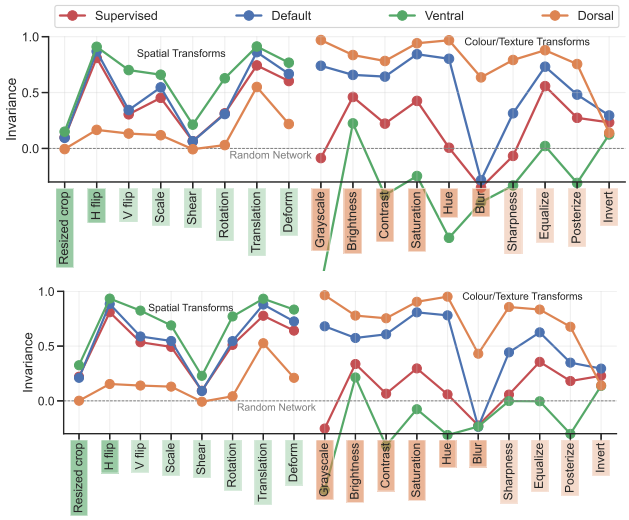

Figure 3. Invariances to synthetic transforms hold for cluttered images from COCO (top) and in-the-wild images from iNaturalist (bottom).

4. Do Contrastive Methods Learn Invariances?

In this section we investigate whether our pre-trained models effectively learn invariance to data augmentations.

Setup We focus on task-agnostic metrics of invariances introduced in Sec 3.2. Other extrinsic measures of invariance like identifiability/classification performance under different transformations are inherently biased towards that task. We therefore use invariance metrics that apply to feature vectors directly. We evaluate our Default, Ventral and Dorsal methods on 1000 images from the ImageNet (ILSVRC12) validation set [15] against a wider array of synthetic augmentation transformations than used for training (Tab 1), but still group these into dorsal and ventral-style transforms.

Results The results in Tab. 2 evaluate the invariance of different transformations at test-time (columns) for the different pre-trained models (rows). We make the following observations. For spatial transformations like rotation and translation, the Ventral model is the most invariant, due to its use of such augmentations during pretraining. Likewise, the Dorsal model has the strongest invariance to transformations in colour and texture, except for the invert transform. The Default model tends to fall in between the two specialised models suggesting strong invariance to any one transformation is traded off for a reasonable variance across the board. The Random model tends to have the highest variance.

While the Ventral model has very low variance to spatial transformations, it has a high variance to colour and texture. Its sensitivity to these transformations is available for solving tasks that depend on colour or texture. Likewise, the Dorsal model is sensitive to spatial information which it could use to solve spatially sensitive tasks. In fact, since the Dorsal model is more spatially sensitive than the Default model, it might achieve better performance on such tasks. We will investigate this in Sec. 6. Overall the results confirm that invariances are indeed learned by contrastive learning with corresponding augmentations. Furthermore, augmentations do tend to increase invariance to other transformations in the corresponding dorsal/ventral family, rather than only the specific subset used for training.

How do invariances change during pre-training? It is clear from the results above that the use of augmentations leads to invariances to those transforms. But how do these invariances change as the model learns? Figure 2 shows how the invariances evolve during pre-training. The results echo those in Table 2, showing the Dorsal and Ventral models quickly specialise to greater corresponding invariances than the default model which has a moderate invariance to all transforms. In terms of the temporal dynamics, while some invariances stabilise quickly, other are continuing to increase at 200 epochs. This suggests that longer training may lead to further increases in invariance, and may explain why several state of the art learners achieve best performance with a very large number of iterations [5, 6].

Do learned invariances hold for uncurated images? We also evaluate the invariance to synthetic transforms on 100 images from the MS COCO val2017 set [36] and iNaturalist 2021 validation set [51]. As can be seen in Fig. 3, the invariances of all models match those in Fig. 1 (top) on ImageNet, showing that these learned invariances are not limited to highly curated object-centric images, but also to the cluttered images of COCO and the in-the-wild nature of iNaturalist.

5. Do Learned Synthetic Invariances Provide Invariance to Real-World Transforms?

We have shown how the use of certain augmentations lead to features that are substantially invariant to those augmentations, as well as others in the same dorsal/ventral family. An important question that has not been studied in the literature is whether these learned invariances lead to invariances under real-world transforms, like viewpoint or illumination changes. Does the use of colour augmentations during pretraining lead to features that are invariant to day/night in real images? Does the use of crop/flip augmentation in training lead to pose invariance in real images? While these kinds of questions were intensively studied for classic hand-crafted features [38], they have not been studied for invariances learned by self-supervision.

We address this question from two perspectives: intrinsically, by measuring the invariance of different representations with respect to different real-world transformations;

Table 3. Comparing models in terms of their invariances to real-world transformations.

		Flickr1024	COIL100	ALOI	ALOT	DaLI	ALOI	ALOT	ALOI	ALOT	ExposureErrors	RealBlur
		Stereo	Pose/Scale	Viewpoint	Viewpoint	Deform. & Illumin.	Illumination	Illumination	Temperature	Temperature	Exposure	Blur
Distance		Random	51.22	39.09	32.36	50.83	49.57	33.37	45.99	14.21	41.07	50.14	22.41
		Supervised	27.50	35.40	34.66	43.93	45.99	29.72	40.57	10.18	33.03	25.55	25.87
	↓	Default	19.96	24.20	20.29	**39.96**	34.97	18.53	37.48	6.60	17.34	17.96	19.15
		Ventral	**19.91**	**23.19**	**15.94**	41.80	**33.84**	**15.73**	**37.28**	11.31	54.28	34.45	32.52
		Dorsal	45.37	44.07	38.83	53.62	45.86	30.54	41.63	**4.35**	**8.14**	**13.15**	**10.97**
Similarity		Random	0.62	0.42	0.48	0.24	0.26	0.58	0.44	0.90	0.73	0.41	0.91
		Supervised	0.90	0.70	0.64	0.67	0.56	0.77	0.75	0.97	0.89	0.84	0.89
	↑	Default	**0.94**	0.75	0.77	0.70	0.60	0.84	0.76	0.98	0.97	0.90	0.90
		Ventral	**0.94**	**0.84**	**0.88**	**0.72**	**0.69**	**0.90**	**0.80**	0.94	0.78	0.69	0.82
		Dorsal	0.74	0.54	0.64	0.32	0.46	0.79	0.61	**1.00**	**0.99**	**0.96**	**0.98**

and extrinsically, by quantifying how well features trained for different synthetic invariances can be used to predict known real-world transformations.

5.1. Intrinsic Invariance Measurements

Experimental Details We use the same metrics introduced in Section 4, but instead of using synthetic transformations typically used in data augmentation schemes, we collect a suite of datasets that exhibit known real-world transformations: **Flickr1024** [48] contains stereo image pairs. We use this to measure invariance to small lateral changes in viewpoint. **COIL-100** [39] is a dataset of 7,200 images of 100 objects photographed under varying pose conditions against a black background. Each object is imaged at every 5 degree angle of rotation around the vertical axis resulting in 72 images. This creates a suitable dataset for us to investigate the real-world viewpoint invariance of our models. **ALOI** [22] contains 1,000 objects captured under varying poses, camera angles and lighting conditions, allowing measurements of both viewpoint and illumination invariance. **ALOT** [4] is a similar dataset in structure but contains photos of 250 textures instead of objects. **DaLI** [50] consists of 12 objects photographed under different deformations and lightning conditions. **ExposureErrors** [1] is composed of 24,000 images rendered at different exposures from raw RGB data. **RealBlur** [45] has 4,500 geometrically aligned pairs of blurred and sharp images, thereby providing an ideal setup for measuring real-world blur invariance.

In contrast to the experimental setup in Section 4, we do not have an untransformed reference image. Instead, we consider all pairs of images for a given object/scene/-texture within each dataset (or subset of the dataset for ALOI/ALOT), and average our metrics across pairs. For example in the case of viewing angle variation in COIL-100, a fully pose invariant feature would exhibit full similarity/zero distance across all corresponding image pairs.

Results The results in Table 3 group the benchmarks datasets according to whether they exhibit ventral-like or dorsal-like real-world translations. The DaLI benchmark mixes both flavours of transformations, so we colour it separately. From the results we can see that our models have learned strong real-world invariances in many cases. For example the ventral model has maximum similarity for all the (green) ventral-like transformations. However, this is less consistent for the dorsal model as it shows lower invariance to illumination on the ALOI/ALOT/DaLI datasets. That a model trained with crops and flips achieves stronger illumination invariance than one trained with colour augmentations is surprising and highlights the importance of understanding the role of data augmentation better in representation learning.

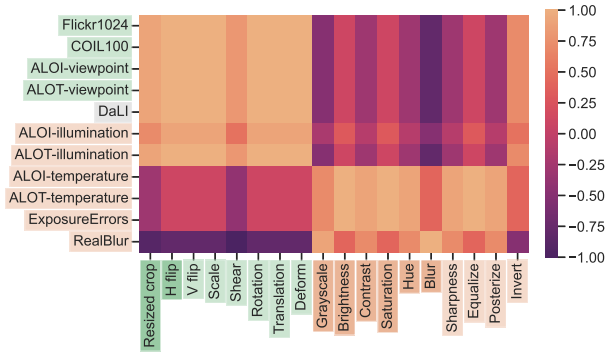

Figure 4. Rank correlation between invariances to synthetic and real-world transforms. Invariance to synthetic transforms is highly correlated with invariance to the corresponding family of real-world transforms.

Summary In summary, to answer the question of whether learned invariances to synthetic transforms translates to learned invariances to real-world transforms, we report in Figure 4 the rank correlation (over our five models) between all pairs of synthetic and real-world invariances considered. From the results we can see a clear block structure that strong invariance to dorsal-like synthetic transforms correlates with the dorsal-like real-world transforms, and vice-versa. The only exception to this is that data with real-world illumination changes exhibits stronger correlation with ventral-style synthetic transforms.

Table 4. Comparing models learned invariances on Causal3DIdent. Regression R^2 fit when predicting parameters from features. Our Dorsal model is highly sensitive to ventral-style transforms and our Ventral model highly sensitive to dorsal-style transforms. Our fused models exhibit strong predictive capability across the board.

	Obj. Pos. x	Obj. Pos. y	Obj. Pos. z	Obj. Rot. x	Obj. Rot. y	Obj. Rot. z	Spot. Pos.	Obj. Colour	Spot. Colour	Bkg. Colour
Ventral	0.89	0.91	0.84	0.66	0.67	0.62	0.92	**0.93**	**0.91**	**1.00**
Dorsal	0.94	**0.97**	0.91	0.80	0.84	0.79	0.95	0.56	0.22	0.88
Ven+Dor	0.94	**0.97**	0.91	0.80	0.82	0.77	0.95	0.92	0.90	**1.00**
Def+Ven+Dor	**0.95**	**0.97**	**0.94**	**0.87**	**0.89**	**0.85**	**0.96**	0.92	0.89	**1.00**

5.2. Extrinsic Invariance Measurements

To provide a different perspective on invariance to real-world transforms, we evaluate our features on Causal3DIdent benchmark. In particular, we follow [52] in regressing real-world variables such as pose, object colour, light colour, etc from our features. A feature with complete spatial invariance would fail to predict pose, while one with complete colour invariance would fail to predict colour, etc.

Setup We use kernel ridge regression with an RBF kernel, sample 20,480 training points and 40,960 test points and standardise images and targets. As the feature dimensionality of our models is much greater than of those in [52], we expand the hyperparameter search space for α and γ to $[0.0001, 0.001, 0.01, 0.1, 1]$ and $[0.00001, 0.0001, 0.001, 0.01, 0.1, 1, 10, 100]$, respectively.

Results From the results in Table 4 we see that this evaluation paradigm also confirms that learned invariances translate to some extent to real transformations. The dorsal model obtains better performance on the pose prediction tasks, while the ventral model obtains better performance on the colour prediction tasks.

6. Do Different Downstream Tasks Benefit From Different Invariances?

In the previous sections we have showed how contrastive training under data augmentation learns invariance to synthetic and real-world transformations. It also confirmed the colour/texture sensitivity of the Ventral model and the spatial sensitivity of the Dorsal model. The Default model was found to always fall in between the two more specialised learners, with weaker invariance than one alternative but stronger than the other. In terms of real-world benchmarks, self-supervised methods are widely evaluated on ImageNet recognition, with the literature having a lesser focus and lack of consistency in evaluation of other non-recognition tasks. Since the default augmentations are largely chosen to optimise recognition benchmarks, there is a chance that it may be overfit to these tasks and perform less well on others. We therefore investigate how learned invariances affect a more diverse suite of real downstream tasks of interest, hypothesising that different features may be preferred, depending on the (in)variance needs of each downstream task.

Experimental Details Our suite of downstream tasks consists of object recognition on standard benchmarks **CIFAR10** [32], **Caltech101** [20] and **Flowers** [40]; as well as a set of spatially sensitive tasks including facial landmark detection on **300W** [47] and **CelebA** [37], and pose estimation on **Leeds Sports Pose** [30]. We freeze the backbones and extract features from just after the average pooling layer of the ResNet50 architectures. We fit a ridge or logistic regression model on these features, depending on the task in question. To tune the $\ell 2$ regularisation value we perform 5-fold cross-validation over a grid of 45 logarithmically spaced values between 10^{-6} to 10^{5}, following [6, 18]. After finding the optimal hyperparameter choice, the model is retrained on the full training set and evaluated on the test set. We report accuracies (between 0 and 1) for classification tasks and R^2 values for regression tasks. For comparison we also evaluate random and supervised backbones.

Results Table 5 shows the linear readout performance on all tasks considered. On the datasets most similar to ImageNet: CIFAR10, Caltech101 and Flowers, the Default or Supervised models achieve the highest classification accuracy, followed by the Ventral and then the Dorsal model. On the spatially sensitive tasks the Dorsal model outperforms the Ventral model substantively, with the Dorsal model performing best overall on 300W. These results show some evidence that the Default (and to a lesser extent Ventral model) model is well suited for object recognition on ImageNet-like datasets, but both are weak in comparison to a model with more spatial sensitivity when solving the pose-related tasks. Overall this supports the hypothesis that different (in)variances are required for best performance on different types of tasks.

Improving Performance Through Feature Fusion Our previous analyses show that different real-world tasks prefer different invariances. The default model tries to satisfy them all by using a mix of augmentations to obtain a moderate amount of invariance to all transformations (Sec 4), but dorsal/ventral specialised features can be better for particular tasks (Table 5, above). We therefore explore whether a fusion of specialised features can perform competitively across the board. In particular we explore Ventral-Dorsal fusion, as well as three way Default-Ventral-Dorsal fusion.

Experimental Details The evaluation follows the setup de-

Table 5. Downstream performances of our models. The differing performances in the tasks showcases how the Ventral and Dorsal models capture important but *different* properties necessary for wide transfer. Random refers to a randomly initialised feature extractor and '+' refers to feature concatenation. On the left datasets we report the classification accuracy and on the right the R^2 regression metric. Row colours indicate whether dorsal or ventral turned out better for the given task.

	CIFAR10	Caltech101	Flowers	300W	CelebA	LSPose	Avg.
Random	0.38	0.19	0.23	0.22	0.43	0.09	0.26
Supervised	**0.90**	**0.89**	0.85	0.15	0.49	0.18	0.58
Default	0.89	0.86	**0.87**	0.45	0.60	**0.26**	**0.65**
Ventral	0.82	0.61	0.77	0.10	0.49	0.20	0.50
Dorsal	0.72	0.53	0.21	**0.63**	**0.62**	0.25	0.49
Default($\times$3)	**0.92**	**0.89**	**0.89**	0.35	0.65	0.29	0.67
Ven+Dor	0.85	0.73	0.75	0.56	0.64	0.29	0.64
Def+Ven+Dor	0.90	0.86	0.87	**0.60**	**0.68**	**0.32**	**0.71**

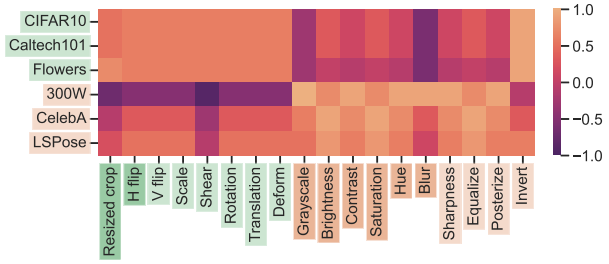

Figure 5. Rank correlation between synthetic invariances and downstream tasks of our set of models in Table 5 (top). A high value between a transform and task means that learning a stronger invariance to the transform is highly correlated with getting better at the task.

scribed above, but as our fused representations have higher dimensionality, we shift the $\ell 2$ search space for Ven+Dor to 10^{-5} to 10^{6} and Def+Ven+Dor 10^{-4} to 10^{7}. Finally, to compare the concatenated features of Def+Ven+Dor, we evaluate a second Default model with a $3\times$ wider architecture – ResNet50($\times$3) – which was trained with MoCo-v2 for 200 epochs on ImageNet like our other models and uses the same hyperparameter search space as Def+Ven+Dor.

Results From the results in Table 6 (bottom) and Table 4 (bottom), we can see that the Ven+Dor model and Def+Ven+Dor fusion models perform strongly across the board. While the Default($\times$3) model is unsurprisingly best for recognition tasks, this is only by a small margin; while the 3-way fusion is dramatically better for 300W, and the most consistent performer across the board.

This result is particularly interesting, as a goal of self-supervised learning is to provide a single feature that provides excellent performance for diverse downstream tasks. While we showed the default model falls down in this regard, our fused feature provides reliable performance across the board. We therefore recommend it to practitioners who want a single feature with which to perform diverse tasks.

7. Discussion

We have performed the first thorough evaluation of self-supervised learning in terms of augmentations used for training, and resulting downstream invariance and task impact. In particular we showed that: (1) CNNs trained contrastively do largely learn invariances corresponding to the augmentations used. However, specialising CNNs to particular dorsal/ventral augmentations can lead to greater corresponding invariances (Table 2). (2) The learned invariances to synthetic transforms do provide some degree of invariance to corresponding real-world transforms (Table 3, Fig 4). (3) Different real-world downstream tasks do prefer features providing different invariances (Table 5), and invariance-specialised features can sometimes outperform the standard default augmentation for spatially sensitive tasks. (4) Fusing features tuned for different types of invariances provides a consistently high performing strategy (Table 5). This outperforms the default model on pose related tasks, suggesting that it was over-tuned for recognition. Our feature ensemble strategy is promising for providing high performance *general purpose* real-world features. Collectively based on these results we encourage the SSL community to evaluate on more diverse downstream task types.

Limitations and Future Work Our study is limited in only evaluating MoCo and CNNs as a base learner. We expect results would be qualitatively similar for related methods, including related non-contrastive learners [9, 57] and transformer architectures [16], but this remains to be confirmed.

Acknowledgements

This work was supported by the Engineering and Physical Sciences Research Council (EPSRC) Grant number EP/S000631/1; and the MOD University Defence Research Collaboration (UDRC) in Signal Processing.

References

[1] Mahmoud Afifi, Konstantinos G. Derpanis, Björn Ommer, and Michael S. Brown. Learning Multi-Scale Photo Exposure Correction. In *CVPR*, 2021. 6

[2] Shahab Bakhtiari, Patrick Mineault, Tim Lillicrap, Christopher C. Pack, and Blake A. Richards. The functional specialization of visual cortex emerges from training parallel pathways with self-supervised predictive learning. *bioRxiv*, 2021. 3

[3] Valerio Biscione and Jeffrey Bowers. Learning Translation Invariance in CNNs. In *2nd Workshop on Shared Visual Representations in Human and Machine Intelligence (SVRHM), NeurIPS*, 2020. 3

[4] Gertjan J Burghouts and Jan-Mark Geusebroek. Material-specific adaptation of color invariant features. *Pattern Recognition Letters*, 2009. 6

[5] Mathilde Caron, Ishan Misra, Julien Mairal, Priya Goyal, Piotr Bojanowski, and Armand Joulin. Unsupervised Learning of Visual Features by Contrasting Cluster Assignments. In *NeurIPS*, 2020. 5

[6] Ting Chen, Simon Kornblith, Mohammad Norouzi, and Geoffrey Hinton. A Simple Framework for Contrastive Learning of Visual Representations. In *ICML*, 2020. 2, 3, 4, 5, 7, 12

[7] Ting Chen, Simon Kornblith, Kevin Swersky, Mohammad Norouzi, and Geoffrey Hinton. Big Self-Supervised Models are Strong Semi-Supervised Learners. In *NeurIPS*, 2020. 1, 2, 4

[8] Xinlei Chen, Haoqi Fan, Ross Girshick, and Kaiming He. Improved Baselines with Momentum Contrastive Learning. *arXiv*, 2020. 2, 3, 4, 11

[9] Xinlei Chen and Kaiming He. Exploring Simple Siamese Representation Learning. In *CVPR*, 2021. 1, 8

[10] Taco S. Cohen, Maurice Weiler, Berkay Kicanaoglu, and Max Welling. Gauge Equivariant Convolutional Networks and the Icosahedral CNN. In *ICML*, 2019. 3

[11] Taco S. Cohen and Max Welling. Group Equivariant Convolutional Networks. In *ICML*, 2016. 3

[12] Michael J Cree, John A Perrone, Gehan Anthonys, Aden C Garnett, and Henry Gouk. Estimating heading direction from monocular video sequences using biologically-based sensors. In *IVCNZ*, 2016. 3

[13] Ekin D. Cubuk, Barret Zoph, Dandelion Mane, Vijay Vasudevan, and Quoc V. Le. AutoAugment: Learning Augmentation Policies from Data. In *CVPR*. IEEE Computer Society, 5 2019. 3

[14] Ekin D. Cubuk, Barret Zoph, Jonathon Shlens, and Quoc V. Le. RandAugment: Practical automated data augmentation with a reduced search space. In *NeurIPS*. IEEE Computer Society, 9 2020. 1

[15] J Deng, W Dong, R Socher, L.-J. Li, K Li, and L Fei-Fei. ImageNet: A Large-Scale Hierarchical Image Database. In *CVPR*, 2009. 2, 4, 5

[16] Alexey Dosovitskiy, Lucas Beyer, Alexander Kolesnikov, Dirk Weissenborn, Xiaohua Zhai, Thomas Unterthiner, Mostafa Dehghani, Matthias Minderer, Georg Heigold, Sylvain Gelly, Jakob Uszkoreit, and Neil Houlsby. An Image is Worth 16x16 Words: Transformers for Image Recognition at Scale. In *ICLR*, 2021. 8

[17] Mohammad K. Ebrahimpour, Jiayun Li, Yen-Yun Yu, Jackson L. Reese, Azadeh Moghtaderi, Ming-Hsuan Yang, and David C. Noelle. Ventral-Dorsal Neural Networks: Object Detection via Selective Attention. In *WACV*. Institute of Electrical and Electronics Engineers Inc., 5 2019. 3

[18] Linus Ericsson, Henry Gouk, and Timothy M. Hospedales. How Well Do Self-Supervised Models Transfer? In *CVPR*, 2021. 2, 7

[19] Linus Ericsson, Henry Gouk, Chen Change Loy, and Timothy M Hospedales. Self-supervised representation learning: Introduction, advances and challenges. *arXiv*, 2021. 2

[20] Li Fei-Fei, Rob Fergus, and Pietro Perona. Learning generative visual models from few training examples: An incremental bayesian approach tested on 101 object categories. In *CVPR Workshops*, 2004. 7, 12

[21] Kunihiko Fukushima. Neocognitron: A self-organizing neural network model for a mechanism of pattern recognition unaffected by shift in position. *Biological Cybernetics*, 1980. 2

[22] Jan-Mark Geusebroek, Gertjan J. Burghouts, and Arnold W.M. Smeulders. The Amsterdam Library of Object Images. *International Journal of Computer Vision*, 2005. 6

[23] Melvyn A. Goodale and A. David Milner. Separate visual pathways for perception and action. *Trends in Neurosciences*, 1992. 2, 3

[24] Ian J Goodfellow, Quoc V Le, Andrew M Saxe, Honglak Lee, and Andrew Y Ng. Measuring Invariances in Deep Networks. In *NeurIPS*, 2009. 3, 4

[25] Jean-Bastien Grill, Florian Strub, Florent Altché, Corentin Tallec, Pierre H. Richemond, Elena Buchatskaya, Carl Doersch, Bernardo Avila Pires, Zhaohan Daniel Guo, Mohammad Gheshlaghi Azar, Bilal Piot, Koray Kavukcuoglu, Rémi Munos, and Michal Valko. Bootstrap Your Own Latent: A New Approach to Self-Supervised Learning. In *NeurIPS*, 2020. 1, 2, 4

[26] Kaiming He, Haoqi Fan, Yuxin Wu, Saining Xie, and Ross Girshick. Momentum Contrast for Unsupervised Visual Representation Learning. In *CVPR*, 2019. 1, 2, 3

[27] Kaiming He, Xiangyu Zhang, Shaoqing Ren, and Jian Sun. Deep residual learning for image recognition. In *CVPR*, 2016. 2, 4

[28] Eric Jang, Sudheendra Vijayanarasimhan, Peter Pastor, Julian Ibarz, and Sergey Levine. End-to-End Learning of Semantic Grasping. In *CoRL*, 2017. 3

[29] Longlong Jing and Yingli Tian. Self-supervised Visual Feature Learning with Deep Neural Networks: A Survey. *IEEE Transactions on Pattern Analysis and Machine Intelligence*, 2020. 2

[30] Sam Johnson and Mark Everingham. Clustered Pose and Nonlinear Appearance Models for Human Pose Estimation. In *BMVC*, 2010. 7, 12

[31] Osman Semih Kayhan and Jan C. van Gemert. On Translation Invariance in CNNs: Convolutional Layers can Exploit Absolute Spatial Location. In *CVPR*, 2020. 3

[32] Alex Krizhevsky and Geoffrey Hinton. Learning Multiple Layers of Features from Tiny Images. *arXiv*, 2009. 7, 12

[33] Alex Krizhevsky, Ilya Sutskever, and Geoffrey E Hinton. ImageNet Classification with Deep Convolutional Neural Networks. In *NeurIPS*, 2012. 2

[34] N. Kruger, P. Janssen, S. Kalkan, M. Lappe, A. Leonardis, J. Piater, A. J. Rodriguez-Sanchez, and L. Wiskott. Deep hierarchies in the primate visual cortex: What can we learn for computer vision? *IEEE Transactions on Pattern Analysis and Machine Intelligence*, 2013. 2, 3

[35] Junnan Li, Pan Zhou, Caiming Xiong, Richard Socher, and Steven C. H. Hoi. Prototypical Contrastive Learning of Unsupervised Representations. In *ICLR*, 2021. 4

[36] Tsung Yi Lin, Michael Maire, Serge Belongie, James Hays, Pietro Perona, Deva Ramanan, Piotr Dollár, and C. Lawrence Zitnick. Microsoft COCO: Common objects in context. In *ECCV*, 2014. 5

[37] Ziwei Liu, Ping Luo, Xiaogang Wang, and Xiaoou Tang. Deep learning face attributes in the wild. In *ICCV*, 2015. 7, 12

[38] K. Mikolajczyk and C. Schmid. A performance evaluation of local descriptors. *IEEE Transactions on Pattern Analysis and Machine Intelligence*, 2005. 5

[39] S. A. Nene, S. K. Nayar, and H. Murase. Columbia Object Image Library (COIL100). Technical report, 1996. 6

[40] Maria Elena Nilsback and Andrew Zisserman. Automated flower classification over a large number of classes. In *Indian Conference on Computer Vision, Graphics and Image Processing (ICVGIP)*, 2008. 7, 12

[41] Aaron van den Oord, Oriol Vinyals, and Koray Kavukcuoglu. Neural Discrete Representation Learning. *NeurIPS*, 2017. 3

[42] Adam Paszke, Sam Gross, Francisco Massa, Adam Lerer, James Bradbury, Gregory Chanan, Trevor Killeen, Zeming Lin, Natalia Gimelshein, Luca Antiga, Alban Desmaison, Andreas Kopf, Edward Yang, Zachary DeVito, Martin Raison, Alykhan Tejani, Sasank Chilamkurthy, Benoit Steiner, Lu Fang, Junjie Bai, and Soumith Chintala. PyTorch: An Imperative Style, High-Performance Deep Learning Library. In *NeurIPS*, 2019. 11

[43] John A. Perrone, Michael J. Cree, and Mohammad Hedayati. Using the properties of primate motion sensitive neurons to extract camera motion and depth from brief 2-d monocular image sequences. In *CAIP*, 2019. 3

[44] Senthil Purushwalkam and Abhinav Gupta. Demystifying Contrastive Self-Supervised Learning: Invariances, Augmentations and Dataset Biases. *arXiv*, 2020. 3

[45] Jaesung Rim, Haeyun Lee, Jucheol Won, and Sunghyun Cho. Real-World Blur Dataset for Learning and Benchmarking Deblurring Algorithms. In *ECCV*, 2020. 6

[46] Sara Sabour, Nicholas Frosst, and Geoffrey E Hinton. Dynamic Routing Between Capsules. *NeurIPS*, 2017. 3

[47] Christos Sagonas, Epameinondas Antonakos, Georgios Tzimiropoulos, Stefanos Zafeiriou, and Maja Pantic. 300 Faces In-The-Wild Challenge. *Image and Vision Computing*, 2016. 7, 12

[48] Daniel Scharstein, Heiko Hirschmüller, York Kitajima, Greg Krathwohl, Nera Nešić, Xi Wang, and Porter Westling. High-Resolution Stereo Datasets with Subpixel-Accurate Ground Truth. In *GCPR*, 2014. 6

[49] Connor Shorten and Taghi M. Khoshgoftaar. A survey on Image Data Augmentation for Deep Learning. *Journal of Big Data*, 2019. 1

[50] Edgar Simo-Serra, Carme Torras, and Francesc Moreno-Noguer. DaLI: Deformation and Light Invariant Descriptor. *International Journal of Computer Vision*, 2015. 6

[51] Grant Van Horn, Elijah Cole, Sara Beery, Kimberly Wilber, Serge Belongie, and Oisin Mac Aodha. Benchmarking Representation Learning for Natural World Image Collections. In *CVPR*, 2021. 5

[52] Julius von Kügelgen, Yash Sharma, Luigi Gresele, Wieland Brendel, Bernhard Schölkopf, Michel Besserve, and Francesco Locatello. Self-Supervised Learning with Data Augmentations Provably Isolates Content from Style. In *NeurIPS*, 2021. 3, 7

[53] Tongzhou Wang and Phillip Isola. Understanding Contrastive Representation Learning through Alignment and Uniformity on the Hypersphere. In *ICML*, 2020. 2

[54] Zixin Wen and Yuanzhi Li. Toward Understanding the Feature Learning Process of Self-supervised Contrastive Learning. *arXiv*, 2021. 3

[55] Tete Xiao, Xiaolong Wang, Alexei A. Efros, and Trevor Darrell. What Should Not Be Contrastive in Contrastive Learning. In *ICLR*, 2021. 3

[56] Nabeel Younus Khan, Brendan McCane, and Geoff Wyvill. SIFT and SURF Performance Evaluation Against Various Image Deformations on Benchmark Dataset. In *International Conference on Digital Image Computing: Techniques and Applications*, 2011. 2

[57] Jure Zbontar, Li Jing, Ishan Misra, Yann LeCun, and Stéphane Deny. Barlow Twins: Self-Supervised Learning via Redundancy Reduction. In *ICML*, 2021. 2, 8

A. Data augmentation for pre-training

We use the strong contrastive baseline MoCo-v2 [8] for pre-training our models and use its augmentation policy as our basis for our experiments. Our Default model is trained using the full set of augmentations detailed below in PyTorch [42] code.

```
transforms.Compose([
    transforms.RandomResizedCrop(224, scale=(0.2, 1.)),
    transforms.RandomApply([
        transforms.ColorJitter(0.4, 0.4, 0.4, 0.1)
    ], p=0.8),
    transforms.RandomGrayscale(p=0.2),
    transforms.RandomApply([moco.loader.GaussianBlur([.1, 2.])], p=0.5),
    transforms.RandomHorizontalFlip(),
    transforms.ToTensor(),
    transforms.Normalize(mean=[0.485, 0.456, 0.406], std=[0.229, 0.224, 0.225])
])
```

Listing 1. Default augmentation policy

The Ventral model only uses resized crops and horizontal flips.

```
transforms.Compose([
    transforms.RandomResizedCrop(224, scale=(0.2, 1.)),
    transforms.RandomHorizontalFlip(),
    transforms.ToTensor(),
    transforms.Normalize(mean=[0.485, 0.456, 0.406], std=[0.229, 0.224, 0.225])
])
```

Listing 2. Ventral augmentation policy

And finally the Dorsal model uses grayscale, color jitter and blurring.

```
transforms.Compose([
    transforms.Resize(224),
    transforms.CenterCrop(224),
    transforms.RandomApply([
        transforms.ColorJitter(0.4, 0.4, 0.4, 0.1)
    ], p=0.8),
    transforms.RandomGrayscale(p=0.2),
    transforms.RandomApply([moco.loader.GaussianBlur([.1, 2.])], p=0.5),
    transforms.ToTensor(),
    transforms.Normalize(mean=[0.485, 0.456, 0.406], std=[0.229, 0.224, 0.225])
])
```

Listing 3. Dorsal augmentation policy

B. Synthetic transforms

For Table 2 we compute the invariance metrics based on the following synthetic transforms.

- Resized crop: We generate 256 crops with anchor points positioned between 0 and 64 pixels from the top and left of the original image (of size 256×256). A crop is between 25% and 75% of the image in both height and width. After, the crop is resized to 224×224.
- Horizontal flip: A single horizontally flipped image is generated in addition to the unaugmented image.
- Vertical flip: A single vertically flipped image is generated in addition to the unaugmented image.
- Scale: We generate 256 images rescaled between $\frac{1}{4}$ to 2 times its original size.
- Shear: We generate 256 images with horizontal and vertical shear of -160 to 160 degrees.
- Rotation: We generate 256 images with rotation angles between 0 and 360 degrees.
- Translation: We generate 256 images with horizontal and vertical translation of -16 to 16 pixels.
- Deform: We generate 256 images with the ElasticTransform function of the albumentations package, with σ between 10 and 50.
- Grayscale: A single grayscale image is generated in addition to the unaugmented image.
- Brightness: We generate 256 images where brightness is $\frac{1}{4}$ to 5 times its original value.
- Contrast: We generate 256 images where contrast is $\frac{1}{4}$ to 5 times its original value.
- Saturation: We generate 256 images where saturation is $\frac{1}{4}$ to 5 times its original value.
- Hue: We generate 256 images where hue is set to one of 5 values spread over the colour circle.
- Blur: We generate 256 images with Gaussian blur where σ is between 10^{-5} to 20.
- Sharpness: We generate 256 images where the sharpness is adjusted by a factor of 1 to 30.
- Equalize: A single image with an equalized histogram is generated in addition to the unaugmented image.
- Posterize: We generate seven images by reducing the number of bits for each colour channel to 1-7 in addition to the full 8-bit unaugmented image.
- Invert: A single image with inverted colours is generated in addition to the unaugmented image.

C. Downstream evaluation

We use the existing test sets for CIFAR10 [32] [20], Flowers [40] and CelebA [37] and their train (or train+val) sets for cross-validation and training the final model. On Caltech101 we randomly select 30 images per class to form the training set and we test on the rest. On 300W [47] we use both indoor and outdoor sets and join 40% of the images in each set to form a test set. Similarly, for Leeds Sports Pose [30] we use 40% of the images for testing. For both datasets, the rest of the images are used for cross-validation and fitting the final model. For CIFAR10 we report accuracy and for Caltech101 and Flowers, mean per-class accuracy. On 300W and CelebA we perform facial landmark regression and report the R^2 regression metric and for Leeds Sports Pose we perform pose estimation and report R^2.

We follow the evaluation of [6], but additionally perform 5-fold cross-validation for selecting hyperparameters. We extract features from a frozen backbone and, for classification datasets (CIFAR10, Caltech101, Flowers) fit a logistic regression classifier and for regression datasets (300W, CelebA and Leeds Sports Pose) we fit ridge regression. For both settings, the $\ell 2$ hyperparameter search range is 45 logarithmically spaced values between 10^{-6} to 10^{5}. For the larger and fused models we increase shift the range to 10^{-5} to 10^{6} for Ven+Dor and 10^{-4} to 10^{7} for Def+Ven+Dor and Default ($\times 3$).